

Intravoxel incoherent motion diffusion-weighted imaging evaluated the response to concurrent chemoradiotherapy in patients with cervical cancer

Hao Bian, MD^a, Fenghai Liu, MD^{a,*}, Sha Chen, MD^b, Guoce Li, MD^a, Yancheng Song, MD^a, Min Sun, MD^a, Honghuan Dong, MD^a

Abstract

To evaluate the application of multiple b values diffusion-weighted imaging based on biexponential signal decay model to predict the response to concurrent chemoradiotherapy in cervical cancer patients.

This prospective study enrolled 28 patients (mean age: 50.89 ± 10.70 years) with cervical cancer confirmed by biopsy who received concurrent chemoradiotherapy. Pelvic magnetic resonance scans were performed 2 weeks before, 7 days and 21 days after the initiation of therapy, and 1 month after the end of the treatment. Diffusion-weighted imaging with b values of 0, 50, 450, and 850 s/mm^2 were performed, and tumor volume, means of tumor apparent diffusion coefficient (ADC_{min} , ADC_{mean} , ADC_{slow} , ADC_{fast} , and F_{fast} were measured.

Pretreatment ADC_{min} and ADC_{slow} of good outcome group were significantly higher than those of poor outcome group ($P < .05$). At the 7th day of the treatment, F_{fast} and its change rate of good outcome group were significantly higher than those of poor outcome group ($P < .05$). At the 7th day and 21st day of the treatment, F_{fast} showed a slowly increasing tendency with no significant difference compared with pretreatment value in poor outcome group ($P < .05$). One month post-treatment, only ADC_{slow} change rate was significantly higher in good outcome group than that in poor outcome group.

Intravoxel incoherent motion-related ADC values could be utilized to better predict the outcome of cervical cancer chemoradiotherapy.

Abbreviations: ADC = apparent diffusion coefficient, DWI = diffusion-weighted imaging, IVIM = intravoxel incoherent motion, MRI = magnetic resonance imaging, T2WI = T2-weighted imaging.

Keywords: apparent diffusion coefficient, cervical cancer, chemoradiotherapy, diffusion-weighted imaging, intravoxel incoherent motion

1. Introduction

Concurrent chemoradiotherapy is now recognized as the preferred standard for advanced cervical cancer treatment.^[1] Early and reliable evaluation of tumor response to the treatment, timely adjustment of treatment plan, and prevention or reduction of drug toxicity are important to improve patient survival.^[2]

Conventional assessment of tumor therapy response mostly relies on morphological changes in tumor dimension. However, the changes in gross tumor size frequently lag behind cellular changes that occur earlier in responders. In addition, high signal intensity in stroma on T2-weighted image is nonspecific, and makes it difficult to differentiate between residual tumor and radiation changes, especially in the first 3 months after the completion of chemoradiotherapy.^[3]

Diffusion-weighted imaging (DWI) is a unique noninvasive modality that provides image contrast dependent on intravoxel diffusion of water molecules inside the body. Effective therapy-induced apoptosis, necrosis, and increased extracellular space are associated with increased apparent diffusion coefficient (ADC).^[4–6] Recently, several clinical studies have shown the potential of DWI in predicting or monitoring responses to concurrent chemoradiotherapy in cervical cancer. However, monoexponential ADC analysis quantitatively characterized only the overall diffusivity of the tissue in most studies. Intravoxel incoherent motion (IVIM) theory predicts a biexponential model of signal attenuation, with the potential to separately reflect the diffusion of water molecules and perfusion effects.^[7] Recent study showed that perfusion-related parameter derived from IVIM imaging may predict prognosis in head and neck carcinomas.^[8] To the best of our knowledge, no correlation for IVIM parameters during early treatment and prognosis for cervical cancer has been reported.

Editor: Miao Liu.

The authors have no funding and conflicts of interest to disclose.

^aDepartment of Radiology, ^bDepartment of Ultrasound, Cangzhou Central Hospital, Cangzhou, Hebei, China.

*Correspondence: Fenghai Liu, Department of Radiology, Cangzhou Central Hospital, 16 West Xinhua Road, Yunhe District, Cangzhou, Hebei 061001, China (e-mail: lfh600@126.com).

Copyright © 2019 the Author(s). Published by Wolters Kluwer Health, Inc. This is an open access article distributed under the terms of the Creative Commons Attribution-Non Commercial License 4.0 (CCBY-NC), where it is permissible to download, share, remix, transform, and buildup the work provided it is properly cited. The work cannot be used commercially without permission from the journal.

How to cite this article: Bian H, Liu F, Chen S, Li G, Song Y, Sun M, Dong H. Intravoxel incoherent motion diffusion weighted imaging evaluated the response to concurrent chemoradiotherapy in patients with cervical cancer. *Medicine* 2019;98:46(e17943).

Received: 17 April 2019 / Received in final form: 26 September 2019 / Accepted: 15 October 2019

<http://dx.doi.org/10.1097/MD.0000000000017943>

Therefore, this study aimed to investigate the application of multiple b value diffusion-weighted imaging based on biexponential signal decay model to the evaluation of cervical cancer response to concurrent chemoradiotherapy.

2. Materials and methods

2.1. Patient population

This prospective cohort study was approved by Ethics Committee of Cangzhou Central Hospital. In all, 31 consecutive patients with cervical cancer confirmed by biopsy who scheduled to receive concurrent chemoradiotherapy were included in this prospective study from January, 2015 to January, 2016, and they provided informed consent. The inclusion criteria were as follows: primary cervical cancer, no surgery before and after concurrent chemoradiotherapy, and no contraindication to magnetic resonance imaging (MRI). Exclusion criteria were discontinuation of treatment ($n=1$, due to radiation related intestinal fistula) or withdraw of follow-up MRI scans ($n=2$). In all, 28 subjects (mean age, 47.78 years; age range, 31–69 years) including 1 clinically staged as Fédération Internationale de Gynécologie Obstétrique (FIGO) IB, 26 staged as FIGO IIB, and 1 staged as FIGO IIIB were finally enrolled in our study.

2.2. Treatment

All patients were treated with pelvic external beam radiotherapy (EBRT) combined with intracavitary brachytherapy. EBRT was delivered at a daily dose of 180 cGy, 5 times per week, for a total dose of 5040 cGy (28 times in total). Chemotherapy started at the commencement of radiotherapy (day 1) with concurrent weekly cisplatin administration at 40 mg/m². Intracavitary brachytherapy was delivered once a week with a fractional dose of 600 cGy at point A, for a total dose of 3000 cGy (5 times in total).

2.3. Follow-up

Pelvic MRI was performed within 2 weeks before therapy, 7 days and 21 days after the therapy initiated (during treatment), and 1 month after the treatment completed. Tumor residue was determined by cervical biopsy 1 month after the treatment completed. Follow-up evaluation including clinical evaluation (vaginal speculum, cervical palpation, thinprep cytologic test, or cervical biopsy) with or without imaging examinations was performed after the completion of the therapy. Average follow-up was 12.7 months (range 9–25.5 months). Patients were divided into 2 groups based on the final outcome: good prognosis group (without pathological tumor residue, no recurrence or metastases during follow-up) and poor prognosis group (with pathological tumor residue or development of recurrence/metastases).

2.4. Scanning protocol

The patients were imaged using 3.0 T MR scanner (Discovery 750W, GE Healthcare, Milwaukee, WI) with an 8-channel phased-array body coil. Axial diffusion-weighted images were acquired using a single-shot echo-planar imaging (SS-EPI) sequence with the coverage of entire uterus and cervix. Imaging parameters of DWI with multi- b values (0, 50, 200, 450, and 850 s/mm²) were as follows: repetition time (TR)/echo time (TE), 3500/minimum ms; number of excitations (NEX), 8; matrix, 128 × 128; field-of-view (FOV), 24 cm; slice thickness, 5 mm; slice

interval, 0 mm. The routine images included sagittal T2-weighted fast spin-echo (FSE) sequences (TR/TE, 3500/130 ms; slice thickness, 6 mm; slice interval, 0 mm; FOV, 26 cm; matrix, 288 × 224; NEX, 4), axial T2-weighted FSE sequences (TR/TE, 4000/130 ms; slice thickness, 5 mm; FOV, 26 cm; matrix, 320 × 224; NEX, 4), coronal T2-weighted FSE sequences (TR/TE, 4000/130 ms; slice thickness, 6 mm, slice interval, 0 mm; FOV, 30 cm; matrix, 288 × 224; NEX=4), axial T1-weighted FSE sequences (TR/TE, 45/10 ms; slice thickness, 6 mm; slice interval, 1 mm; FOV, 26 cm; matrix, 288 × 192; NEX=2).

2.5. ADC measurement

Image postprocessing was performed using the workstation (GE Healthcare, AW4.5) by 1 radiologist with 5 years' experience in pelvic MRI. Free hand regions of interest (ROIs) (≥ 50 mm²) were manually drawn around entire lesions excluding hemorrhagic, necrotic, or cystic regions on each consecutive tumor slice of ADC maps with reference to corresponding T2-weighted imaging (T2WI). MADC software of workstation was used for the calculation of IVIM-derived parameters. Biexponential equation $S(b)/S(0) = F_{\text{fast}} \exp(-ADC_{\text{fast}}b) + (1 - F_{\text{fast}}) \exp(-ADC_{\text{slow}}b)$ was used for the calculation. Multi b value DWI images were input into the software, and free hand ROIs (≥ 50 mm²) were manually placed within the solid components of tumour. The average values of minimum-ADC, mean-ADC, slow-ADC, fast-ADC, and fast-diffusion fraction (ADC_{min} , ADC_{mean} , ADC_{slow} , ADC_{fast} , and F_{fast} , respectively) obtained from all tumor slices were measured. ROIs were placed on the tissue in the original tumor area recognized from the pretreatment images if there was no visible tumor residue after therapy. ADC change rate after treatment was calculated according to the following equation: $(ADC_{\text{post}} - ADC_{\text{pre}})/ADC_{\text{pre}}$.

2.6. Tumor volume measurement

In the baseline MRI examination, during treatment and 1-month follow-up MRI examination, lesions were manually delineated on each consecutive tumor slices of T2-weighted sequence by 1 radiologist with 5 years' experience in pelvic MRI imaging, then tumor volume was automatically calculated by 3D MIP software on a GE workstation (AW 4.5, GE Healthcare). If tumor was invisible, tumor volume was considered as 0 cm³.

2.7. Statistical analysis

The SPSS for windows 17.0 software was used for statistical analysis. Independent t test was used to compare tumor volume in patients with different outcome. Repeated-measures analysis of variance was used to analyze the changes of ADCs and tumor volume during follow-up. In addition, both intergroup and intragroup comparisons were evaluated by multifactor analysis of variance. P value less than .05 indicated a statistically significant difference.

3. Results

3.1. Treatment outcome

Of the 28 patients, 22 patients presented good prognosis. Other 6 patients presented poor prognosis, 4 had tumor residue at 1-month post-therapy biopsy, 1 developed lumbar vertebrae metastasis confirmed by needle biopsy 3 months after the treatment completed, 1 developed peripheral soft tissue of

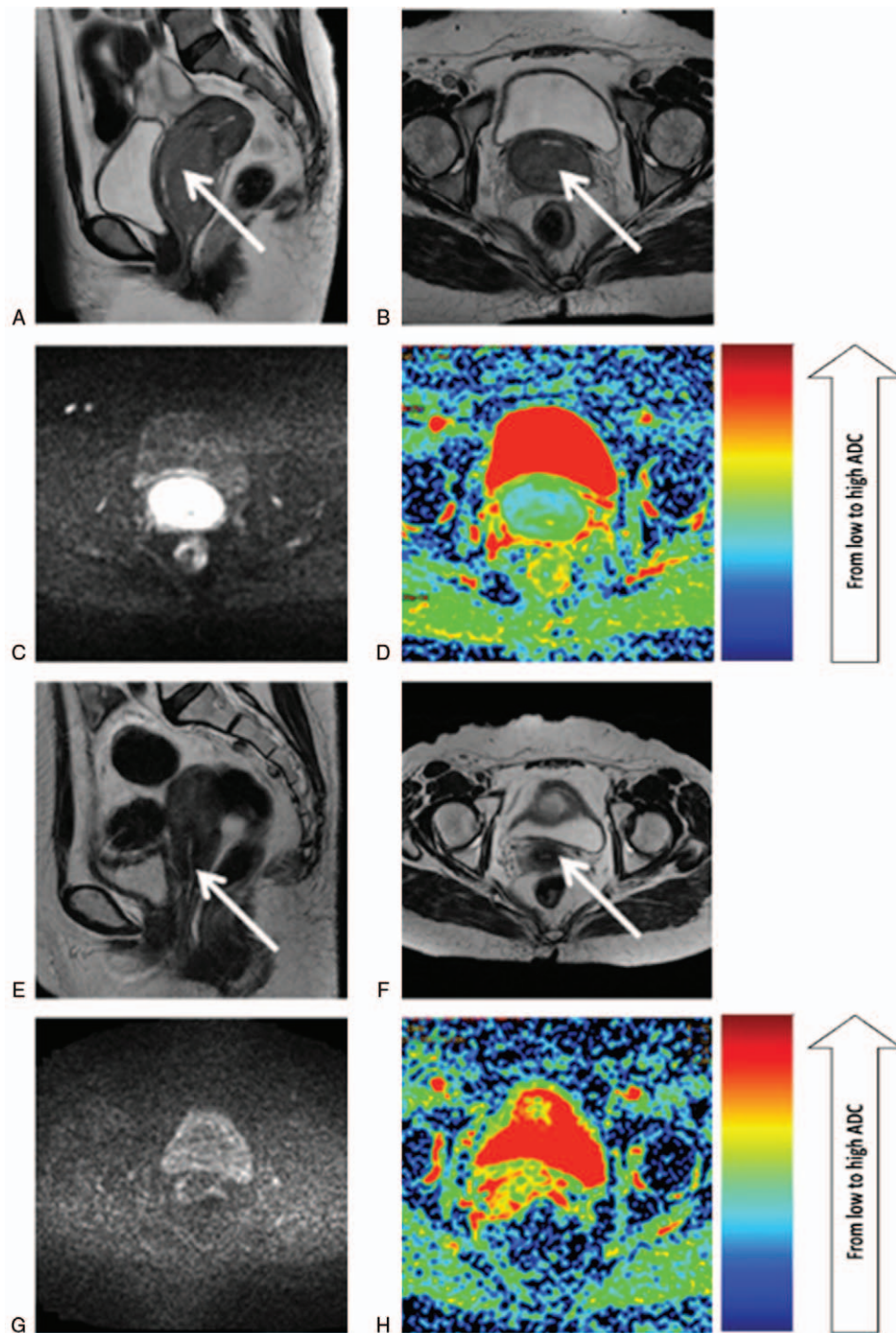


Figure 1. Representative images of good outcome group. A 53-year-old patient with moderately differentiated cervical squamous cell carcinoma (FIGO stage IIB) underwent concurrent chemoradiotherapy. Baseline images before therapy (A–D) and images at 1 month after the end of the therapy (E–H). Sagittal (A) and axial (B) T2-weighted images of cervical cancer showed high signals (white arrow). Axial DWI image with a b value of 850 s/mm^2 showed that tumor had high signal intensity (C). Corresponding ADC map before therapy (D). Sagittal (E) and axial (F) T2-weighted images showed that cervical tumor disappeared after therapy. Axial DWI image with a b value of 850 s/mm^2 showed that cervix had low signal intensity (G). Corresponding ADC map after therapy (H).

urethral orifice metastasis detected by MRI examination 6 months after the treatment completed. Among 4 b values (0, 50, 450, and 850 s/mm^2) used for DWI, the images showed the most significant differences between normal and cancer tissues at b value of 850 s/mm^2 , and the representative images of patients with good and poor prognosis outcome were shown in Figs. 1 and 2, respectively.

3.2. Comparison of tumor volume

There was no statistical difference in tumor volume between 2 groups before therapy ($t=0.115$, $P=.909$). Tumor volume during treatment and tumor-shrinkage rate 1 month after completion of therapy were not significantly different between 2 groups. Only 4 (4/28, 14.3%) patients presented tumor residual

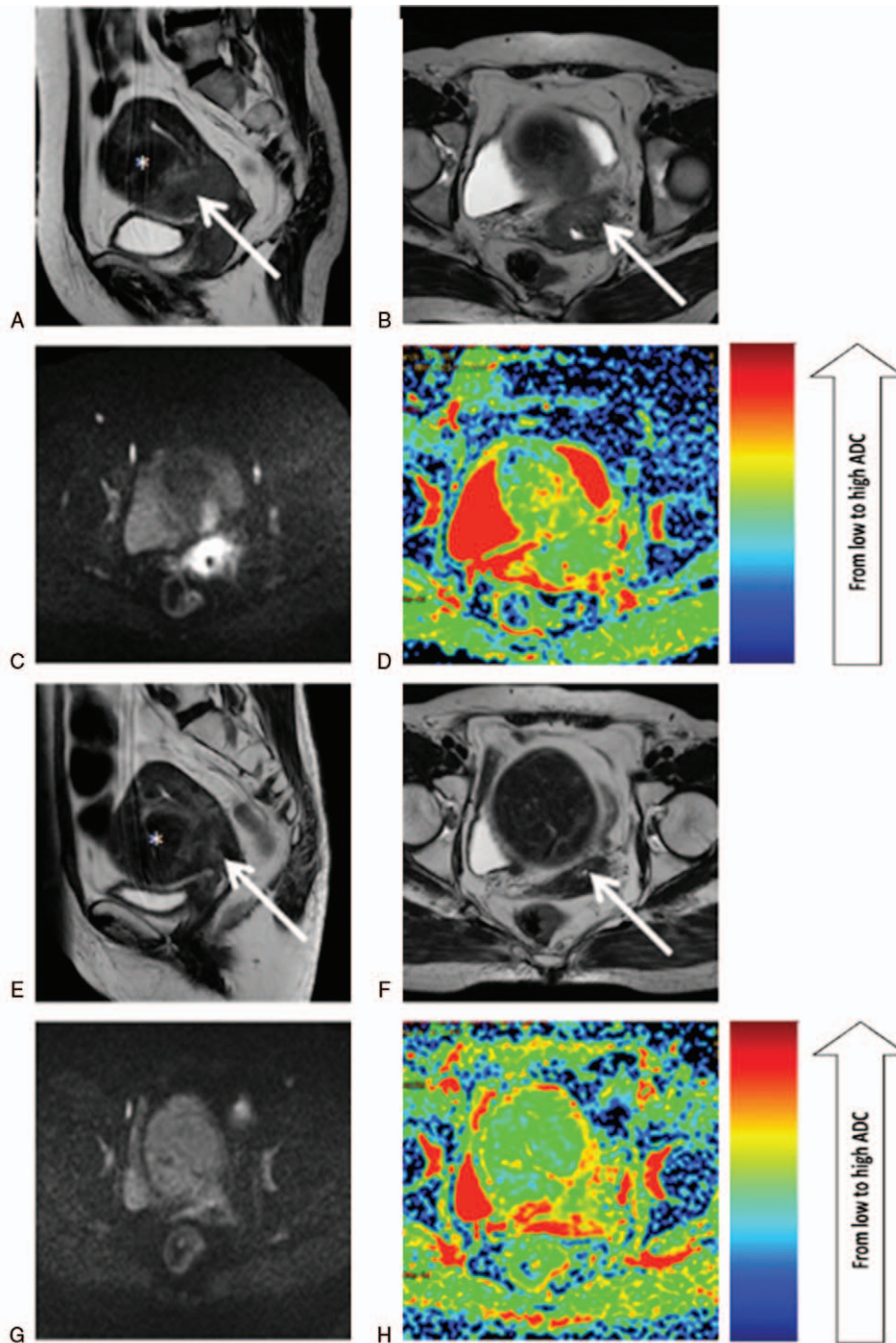


Figure 2. Representative images of poor outcome group. A 64-year-old patient with poorly differentiated cervical squamous cell carcinoma (FIGO stage IIB) combined with multiple fibroids underwent concurrent chemoradiotherapy. Baseline images before therapy (A–D) and images at 1 month after the end of the therapy (E–H). Sagittal (A) and axial (B) T2-weighted images of cervical cancer showed high signals (white arrow) and uterine fibroids showed low signals (*). Axial DWI image with a b value of 850 s/mm^2 showed that tumor had high signal intensity (C). Corresponding ADC map before therapy (D). Sagittal (E) and axial (F) T2-weighted images showed tumor residual after therapy (white arrow). Axial DWI image with a b value of 850 s/mm^2 showed that cervix had low signal intensity (G). Corresponding ADC map after therapy (H).

on their 1-month follow-up MRI images, with the average residual tumor volume of $2.774 \pm 0.543\text{ cm}^3$.

3.3. Comparison of ADC_{min} and ADC_{mean}

The ADC_{min} value before treatment was significantly higher in good prognosis group than in poor prognosis group. However,

there was no statistical difference in pre- ADC_{mean} value between good and poor prognosis group. The changes of ADC_{min} and ADC_{mean} after treatment were both not significantly different between 2 groups. During treatment and 1 month after conclusion of therapy, ADC_{min} and ADC_{mean} continuously elevated, but there was no statistical difference in ADCs for different outcome group. Change rates of ADC_{min} and ADC_{mean}

were not significantly different between 2 groups during follow-up (Tables 1–3).

3.4. Comparison of IVIM-derived parameters

Before treatment, ADC_{slow} was significantly higher in good prognosis group than in poor prognosis group. ADC_{slow} in good prognosis group 21 days after the initiation of therapy was significantly higher than that before treatment. During treatment, ADC_{slow} and the change rates in ADC_{slow} were not significantly different between 2 groups. The change rates in ADC_{slow} of good prognosis group were significantly higher than that of poor group 1 month after the completion of therapy (Tables 1–3).

The ADC_{fast} and the change rates in ADC_{fast} before and after treatment were not significantly different between 2 groups. There was no significant difference in F_{fast} between 2 groups before treatment. F_{fast} and the change rates in F_{fast} were significantly higher in good prognosis group than in poor prognosis group 7 days after the initiation of therapy. F_{fast} in good prognosis group during treatment was significantly higher compared with the baseline F_{fast} . There was no statistical difference in F_{fast} before and after therapy in poor prognosis group, although an increase trend was observed. Both F_{fast} and the change rates in F_{fast} showed no statistically differences between 2 groups 1 month after completion of therapy (Tables 1–3).

4. Discussion

Apparent diffusion coefficient was sensitive to the changes in cellular structure after therapy and could provide an early noninvasive indicator of treatment efficacy.^[9] With the application of EPI sequence, DWI can be used to assess the response of different body tumors to therapy.^[10–12] Several previous studies

have reported the role of pretreatment ADC in predicting therapeutic efficacy for patients with cervical cancer, but the conclusion has not reached a consensus.^[13–16]

In the current study, pretreatment ADC_{min} of cervical cancer patients with good outcome was significantly higher than that of those with poor outcome. ADC_{mean} before therapy did not significantly correlate with tumor response, consistent with previous results.^[13,15,16] Higano et al^[17] found that ADC_{min} was associated with prognosis of malignant astrocytomas. To our knowledge, there was no published report on ADC_{min} -based predicting treatment outcome of cervical cancer.

Signal decay of DWI is influenced not only by molecular diffusion but also by microcapillary diffusion.^[18] IVIM-derived parameters can be obtained with biexponential fitting of multi- b value DWI. Schwarcz et al^[19] speculated that biexponential signal decay could reflect water populations in different binding states. ADC_{fast} was associated with blood velocity, whereas F_{fast} was linked to blood volume in the IVIM model.^[20] It was reported that ADC_{slow} of water molecules in tissues was about $1 \times 10^{-3} \text{ mm}^2/\text{s}$, whereas ADC_{fast} was about $10 \times 10^{-3} \text{ mm}^2/\text{s}$ and $70 \times 10^{-3} \text{ mm}^2/\text{s}$ in the brain and liver, respectively.^[21,22] We speculated that the lowest ADC minimally affected by perfusion contamination, so ADC_{min} similar to ADC_{slow} were significantly different between good and poor outcome groups before therapy.

In this study, ADC_{slow} , ADC_{fast} , and F_{fast} increased in the process of chemoradiotherapy. F_{fast} during treatment in good outcome group were significantly higher compared with pretreatment, whereas F_{fast} gradually increased in poor outcome group, which were not significantly higher than that of pretreatment, may be due to insensitivity to chemoradiotherapy because of continuous hypoperfusion during therapy. Yamashita et al^[23] indicated that well-perfused area of cervical cancer was mainly composed of abundant cancer cell fascicles, whereas

Table 1
Comparison of ADC values in different outcome groups before and 7 days after therapy.

ADCs ($\times 10^{-6} \text{ mm}^2/\text{s}$)	Before therapy		P	7 days after therapy		P
	Good	Poor		Good	Poor	
ADC_{min}	659.4 ± 79.87	556.2 ± 139.4	.025	730.5 ± 93.30	671.3 ± 129.5	.174
ADC_{mean}	977.5 ± 95.42	994.5 ± 216.8	.778	1096.3 ± 74.84	1148.7 ± 161.5	.255
ADC_{fast}	13.76 ± 2.501	12.32 ± 4.001	.174	14.72 ± 1.930	14.40 ± 3.980	.754
ADC_{slow}	784.3 ± 89.00*	673.0 ± 68.59*	.005	824.0 ± 143.9	736.0 ± 49.73	.074
F_{fast}	0.209 ± 0.057	0.223 ± 0.020	.503	0.297 ± 0.064*†	0.241 ± 0.027*	.036

The data are expressed as means ± standard deviations

Good = good outcome group, Poor = poor outcome group

* ADCs were significantly different between good and poor outcome groups at the same time point.

† ADCs were significantly different during or after treatment compared with the baseline in the same group.

Table 2
Comparison of ADC values in different outcome groups 21 days and 1 month after therapy.

ADCs ($\times 10^{-6} \text{ mm}^2/\text{s}$)	21 d after therapy		P	1 mo after therapy		P
	Good	Poor		Good	Poor	
ADC_{min}	1019.3 ± 148.7	849.8 ± 147.8	.056	1022.5 ± 61.57	1014.8 ± 179.3	.870
ADC_{mean}	1391.5 ± 180.4	1263.2 ± 150.2	.065	1511.6 ± 71.90	1537.9 ± 131.5	.499
ADC_{fast}	16.77 ± 2.653*	15.85 ± 5.659	.449	12.63 ± 2.670	11.82 ± 2.469	.488
ADC_{slow}	878.4 ± 143.7*	778.2 ± 72.92	.060	713.2 ± 140.0	799.8 ± 105.8	.100
F_{fast}	0.325 ± 0.083*	0.283 ± 0.084	.202	0.302 ± 0.041*	0.282 ± 0.017*	.318

The data are expressed as means ± standard deviations.

Good = good outcome group, Poor = poor outcome group.

* ADCs were significantly different during or after treatment compared with the baseline in the same group.

Table 3
Change rate of ADCs during and after therapy in different outcome groups.

ΔADC_s	7 d after therapy		<i>P</i>	21 d after therapy		<i>P</i>	1 mo after therapy		<i>P</i>
	Good	Poor		Good	Poor		Good	Poor	
ΔADC_{min}	0.122 ± 0.127	0.102 ± 0.120	.815	0.579 ± 0.304	0.477 ± 0.232	0.588	0.607 ± 0.389	0.677 ± 0.247	0.758
ΔADC_{mean}	0.125 ± 0.055	0.178 ± 0.153	.550	0.428 ± 0.169	0.302 ± 0.205	.315	0.560 ± 0.187	0.608 ± 0.374	.795
ΔADC_{fast}	0.102 ± 0.240	0.184 ± 0.152	.436	0.262 ± 0.342	0.295 ± 0.305	.834	-0.049 ± 0.292	-0.009 ± 0.188	.751
ΔADC_{slow}	0.056 ± 0.163	0.098 ± 0.064	.552	0.123 ± 0.147	0.168 ± 0.170	.529	-0.074 ± 0.254*	0.200 ± 0.209*	.023
ΔF_{fast}	0.478 ± 0.373*	0.092 ± 0.177*	.022	0.597 ± 0.374	0.285 ± 0.409	.087	0.516 ± 0.321	0.269 ± 0.113	.079

The data are expressed as means ± standard deviations.

Good=good outcome group, poor=poor outcome group.

* Change rates of ADCs were significantly different between good and poor outcome group at the same time point.

poorly perfused area was composed of fibrous tissue with scattered cancer cells. It was reported that hypoperfusion volume of cervical cancer derived from DCE imaging before and during therapy significantly predicted unfavorable disease specific survival.^[24] Chandarana et al^[25] found that F_{fast} of renal enhancing masses was significantly higher than that of nonenhancing renal lesions, and there was a correlation between F_{fast} and percent enhancement. Heusch et al^[26] revealed a significant correlation between renal allograft perfusion and F_{fast} originated from IVIM imaging. Thus, F_{fast} can provide information on tissue vascularity.

Vincens et al^[27] suggested that the evaluation of residual tumor 3 to 8 weeks after chemoradiotherapy with MRI was difficult and the risk of false-positive was high. Our study found that change rate of ADC_{slow} 1 month after therapy was helpful to predict the outcome of cervical cancer treatment. Seierstad et al^[28] monitored ADC changes of colorectal tumor model after irradiation and correlated ADC with necrosis and/or edema after irradiation. Therefore, we speculate that the change rate of necrosis may be reflected by different ADC_{slow} between good and poorly outcome groups.

Several limitations of our study should be mentioned. First, sample size was relatively small, especially for cervical cancer patients with poor outcome. Larger cohort study would be required to further verify our results. Second, the follow-up was short. Third, the evaluation of F_{fast} derived from only 4 *b* values may be inaccurate. More *b* values would be recommended in future studies. Fourth, signal intensity of peritumoral edema was similar to that of tumor on T2WI, which may cause an overestimation of tumor volume.

5. Conclusions

In conclusion, our results suggest that compared with anatomical characteristics, IVIM-related ADC values may be utilized to better predict the outcome of cervical cancer patients after chemoradiotherapy, but a prediction model based on these values should be developed to determine the accuracy of the prediction.

Author contributions

Conceptualization: Fenghai Liu.

Investigation: Hao Bian, Sha Chen, Guoce Li, Yancheng Song, Min Sun, Honghuan Dong.

References

[1] Coronel J, Cantu D, Rodriguez-Morales M, et al. Carboplatin and low-dose paclitaxel. An effective regimen in older and comorbid patients with advanced cervical cancer. A phase II study. *Eur J Gynaecol Oncol* 2018;39:997–1001.

[2] Montes FQ, Vázquez-Hernández A, Fenton-Navarro B. Active compounds of medicinal plants, mechanism for antioxidant and beneficial effects. *Phyton Int J Exp Botany* 2019;88:1–10.

[3] Engin G. Cervical cancer: MR imaging findings before, during, and after radiation therapy. *Eur Radiol* 2006;16:313–24.

[4] Kim CK, Park BK, Kim B. Diffusion-weighted MRI at 3 T for the evaluation of prostate cancer. *AJR Am J Roentgenol* 2010;194:1461–9.

[5] Padhani AR, Liu G, Koh DM, et al. Diffusion-weighted magnetic resonance imaging as a cancer biomarker: consensus and recommendations. *Neoplasia* 2009;11:102–25.

[6] Hamstra DA, Rehemtulla A, Ross BD. Diffusion magnetic resonance imaging: a biomarker for treatment response in oncology. *J Clin Oncol* 2007;25:4104–9.

[7] Andreou A, Koh DM, Collins DJ, et al. Measurement reproducibility of perfusion fraction and pseudodiffusion coefficient derived by intravoxel incoherent motion diffusion-weighted MR imaging in normal liver and metastases. *Eur Radiol* 2013;23:428–34.

[8] Hauser T, Essig M, Jensen A, et al. Characterization and therapy monitoring of head and neck carcinomas using diffusion-imaging-based intravoxel incoherent motion parameters preliminary results. *Neuroradiology* 2013;55:527–36.

[9] Chenevert TL, McKeever PE, Ross BD. Monitoring early response of experimental brain tumors to therapy using diffusion magnetic resonance imaging. *Clin Cancer Res* 1997;3:1457–66.

[10] Kim SH, Lee JY, Lee JM, et al. Apparent diffusion coefficient for evaluating tumour response to neoadjuvant chemoradiation therapy for locally advanced rectal cancer. *Eur Radiol* 2011;21:987–95.

[11] Park SH, Moon WK, Cho N, et al. Diffusion-weighted MR imaging: pretreatment prediction of response to neoadjuvant chemotherapy in patients with breast cancer. *Radiology* 2010;257:56–63.

[12] Sun YS, Cui Y, Tang L, et al. Early evaluation of cancer response by a new functional biomarker: apparent diffusion coefficient. *AJR Am J Roentgenol* 2011;197:W23–29.

[13] Rizzo S, Summers P, Raimondi S, et al. Diffusion-weighted MR imaging in assessing cervical tumour response to nonsurgical therapy. *Radiol Med* 2011;116:766–80.

[14] McVeigh PZ, Syed AM, Milosevic M, et al. Diffusion-weighted MRI in cervical cancer. *Eur Radiol* 2008;18:1058–64.

[15] Kim HS, Kim CK, Park BK, et al. Evaluation of therapeutic response to concurrent chemoradiotherapy in patients with cervical cancer using diffusion-weighted MR imaging. *J Magn Reson Imaging* 2013;37:187–93.

[16] Zhang Y, Chen JY, Xie CM, et al. Diffusion-weighted magnetic resonance imaging for prediction of response of advanced cervical cancer to chemoradiation. *J Comput Assist Tomogr* 2011;35:102–7.

[17] Higano S, Yun X, Kumabe T, et al. Malignant astrocytic tumors: clinical importance of apparent diffusion coefficient in prediction of grade and prognosis. *Radiology* 2006;241:839–46.

[18] Le Bihan D, Breton E, Lallemand D, et al. MR imaging of intravoxel incoherent motions: application to diffusion and perfusion in neurologic disorders. *Radiology* 1986;161:401–7.

[19] Schwarcz A, Bogner P, Meric P, et al. The existence of biexponential signal decay in magnetic resonance diffusion-weighted imaging appears to be independent of compartmentalization. *Magn Reson Med* 2004;51:278–85.

[20] Le Bihan D. Intravoxel incoherent motion perfusion MR imaging: a wake-up call. *Radiology* 2008;249:748–52.

- [21] Le Bihan D, Moonen CT, van Zijl PC, et al. Measuring random microscopic motion of water in tissues with MR imaging: a cat brain study. *J Comput Assist Tomogr* 1991;15:19–25.
- [22] Luciani A, Vignaud A, Cavet M, et al. Liver cirrhosis: intravoxel incoherent motion MR imaging: pilot study. *Radiology* 2008;249:891–9.
- [23] Yamashita Y, Baba T, Baba Y, et al. Dynamic contrast-enhanced MR imaging of uterine cervical cancer: pharmacokinetic analysis with histopathologic correlation and its importance in predicting the outcome of radiation therapy. *Radiology* 2000;216:803–9.
- [24] Mayr NA, Huang Z, Wang JZ, et al. Characterizing tumor heterogeneity with functional imaging and quantifying high-risk tumor volume for early prediction of treatment outcome: cervical cancer as a model. *Int J Radiat Oncol Biol Phys* 2012;83:972–9.
- [25] Chandarana H, Lee VS, Hecht E, et al. Comparison of biexponential and monoexponential model of diffusion weighted imaging in evaluation of renal lesions: preliminary experience. *Invest Radiol* 2011;46:285–91.
- [26] Heusch P, Wittsack HJ, Heusner T, et al. Correlation of biexponential diffusion parameters with arterial spin-labeling perfusion MRI: results in transplanted kidneys. *Invest Radiol* 2013;48:140–4.
- [27] Vincens E, Balleyguier C, Rey A, et al. Accuracy of magnetic resonance imaging in predicting residual disease in patients treated for stage IB2/II cervical carcinoma with chemoradiation therapy: correlation of radiologic findings with surgicopathologic results. *Cancer* 2008;113:2158–65.
- [28] Seierstad T, Røe K, Olsen DR. Noninvasive monitoring of radiation-induced treatment response using proton magnetic resonance spectroscopy and diffusion-weighted magnetic resonance imaging in a colorectal tumor model. *Radiother Oncol* 2007;85:187–94.